J Mol Med (2012) 90:837–846
DOI 10.1007/s00109-012-0866-3

ORIGINAL ARTICLE

Structural insights into a human anti-IFN antibody exerting therapeutic potential for systemic lupus erythematosus

Songying Ouyang · Bin Gong · Jin-Zhi Li · Li-Xia Zhao · Wei Wu · Fu-Shun Zhang · Lina Sun · Shu-Jun Wang · Meng Pan · Chuan Li · Wenguang Liang · Neil Shaw · Jie Zheng · Guo-Ping Zhao · Ying Wang · Zhi-Jie Liu · Mifang Liang

Received: 26 October 2011 / Revised: 9 January 2012 / Accepted: 12 January 2012 / Published online: 4 February 2012

Abstract Increasing evidences suggest that the type I interferon α (IFNα) plays a critical role in the etiopathogenesis of systemic lupus erythematosus (SLE), which makes it a promising therapeutic target for the treatment of the disease. By screening a large size non-immune human antibody library, we have developed a human single-chain antibody (ScFv) AIFNα1bScFv01 and corresponding whole antibody AIFNα1bIgG01 to human interferon α1b (IFNα1b) with high specificity and high affinity. The IgG antibody could down-regulate the expression of *ISG15* and *IFIT-1* induced by either recombinant IFNα1b or naïve IFNα from SLE patients' sera, and reduced total serum IgG and IgM antibodies level in a pristane-primed lupus-like mouse model. The crystal structure of AIFNα1bScFv01-IFNα1b complex solved to 2.8 Å resolution revealed that both Pro26-Gln40 region in loop AB and Glu147-Arg150 region in helix E of IFNα1b contribute to binding with AIFNα1bScFv01. Four residues of above two regions (Leu30, Asp32, Asp35 and Arg150) are critical for the formation of antigen–antibody complexes. AIFNα1bScFv01 shares partial epitopes of IFNα1b with its receptor IFNAR2 but with much higher binding affinity to IFNα1b than IFNAR2. Thus, AIFNα1bIgG01 exhibits its neutralizing activity through competition with IFNAR2 to bind with IFNα and prevents the activation of IFNα-mediated signaling pathway. Our results highlight the potential use of the human antibody for modulating the activity of IFNα in SLE.

Keywords Human antibody · IFNα · Crystal structure · Epitope · Systemic lupus erythematosus (SLE)

S. Ouyang, B. Gong, J. Z. Li and L. X. Zhao contributed equally to this work.

S. Ouyang · L.-X. Zhao · W. Liang · N. Shaw · Z.-J. Liu (✉)
National Laboratory of Biomacromolecules,
Institute of Biophysics, Chinese Academy of Sciences,
Beijing 100101, China
e-mail: zjliu@ibp.ac.cn

B. Gong · W. Wu · F.-S. Zhang · L. Sun · C. Li · M. Liang (✉)
National Institute for Viral Diseases Control and Prevention,
China CDC,
Beijing 102206, China
e-mail: mifangl@vip.sina.com

J.-Z. Li · S.-J. Wang · Y. Wang (✉)
Shanghai Institute of Immunology, Institute of Medical Science,
Shanghai Jiaotong University School of Medicine,
Shanghai 200025, China
e-mail: ywang@sibs.ac.cn

M. Pan · J. Zheng
Ruijin Hospital, Shanghai Jiaotong University School of Medicine,
Shanghai 200025, China

G.-P. Zhao · Y. Wang
Shanghai-MOST Key Laboratory for Health and Disease
Genomics, Chinese National Human Genome Center at Shanghai,
Shanghai 201203, China

Introduction

Systemic lupus erythematosus (SLE) is a prototypical, multi-organ autoimmune disease that primarily affects the skin, joints, blood cells, heart, kidneys, and the nervous system [1, 2]. The course of the disease, punctuated with periodic flares and remissions, is unpredictable and is influenced by multiple factors and in some instances by viral infections [3–6]. Currently, there is no efficient and specific

treatment method for SLE. Therefore, the development of new therapeutic strategies for SLE is urgently needed.

Cytokine-mediated immunity plays a crucial role in the pathogenesis of various autoimmune disorders such as SLE [7]. Since human type I interferon α (IFNα) are the main cytokines produced in the very early stage of immune responses, they are extensively engaged in modulation of immunological functions of T cells, B cells and dendritic cells, which are critical for immuno-regulatory effects [8]. However, sustained overproduction of IFNα might break down the peripheral tolerance leading to the occurrence of autoimmune diseases [7, 8]. In recent years, studies on SLE have revealed a central role for IFNα in disease pathogenesis [9]. The features of SLE include unabated production of IFNα in the patients' sera and the overexpression of IFNα-inducible genes in peripheral blood mononuclear cells (PBMCs) [10, 11]. The extent of the increase in IFNα production has a strong correlation with the stages of the disease [12]. These findings implicate the pivotal role of IFNα in the pathogenesis of SLE, leading to the development of IFN-related antagonists as a potential therapeutic intervention in SLE [8, 13].

Therapeutic antibodies targeting IFNα thus become one of the effective ways in the future clinical applications to SLE. Previously report that a humanized IFNα antibody could be used as a therapeutic candidate for insulin-dependent diabetes, SLE, psoriasis and Crohn's disease, which are all characterized by pathological expression of IFNα [14]. Phage antibody display is one of the most widely used methods for the generation of fully human antibodies, while large non-immune and synthetic phage antibody libraries provided the advantage to screen human antibody to human protein [15]. In this report, we describe the generation, characterization and functional analysis of a high affinity human antibody AIFNα1bScFv01 against human IFNα1b in vitro and in vivo. Further, the resolution of a crystal structure of AIFNα1bScFv01-IFNα1b complex provided detailed molecular insights into the interaction of between human neutralizing antibody and IFNα1b.

Materials and methods

Generation of human antibody to IFNα1b and the binding specificity

The ScFv antibody AIFNα1bScFv01 screening process was performed as described previously [16]. The ScFv antibody gene was cloned into whole IgG expression cassette vectors pAc-K-CH3 to generate human IgG antibody AIFNα1-bIgG01 as described previously [17]. The recombinant IgG antibody was expressed in Sf9 insect cells and purified through affinity chromatography. The binding activities of IgG antibodies were analyzed with purified IFNα1b by Western blotting and ELISA as previously described by Gong et al. [18].

BIAcore biosensor assays

For kinetic studies of the interaction and affinity measurement between IFNα1b and AIFNα1bIgG01 antibody by surface plasmon resonance (SPR), a BIAcore biosensor CM5 was used (BIAcore 3000, Sweden). The IFNα1b was immobilized on the sensor chip in 8.3 μg/ml sodium acetate buffer, pH 4.0. Antibody was exposed to the chip at 31.25, 62.5, 125, 250, 500 nM in phosphate-buffered saline supplemented with 0.005% Tween-20. The binding on-rate (Ka) and off-rate (Kd) was measured. The affinity constants of IgG antibody was calculated using the bivalent analyze model included in the BIA evaluation software.

Neutralization tests

For antibody neutralization tests, fresh blood samples from SLE patients and healthy donors were collected and PBMCs from healthy donors were isolated by density gradient centrifugation. The PBMCs were plated at 1×10^5/well in 96-well plates. IFNα1b with gradient concentrations (0, 10, 100 ng/ml) and AIFNα1bIgG01 antibody (0, 3, 12 μg/ml) were added to the plates. In addition of the recombinant IFNα1b, the naïve IFNα from either SLE patients' sera or healthy donors' sera with AIFNα1bIgG01 antibody (24 μg/ml) were added in separate plates. All above plates were incubated at 37°C with 5% CO_2 for 4 h. After incubation, total RNAs were extracted from above PBMCs with TRIzol reagent (Invitrogen, USA) and reverse transcribed to cDNA. Real-time PCR was performed to detect the type I IFN-stimulated genes (ISGs), *ISG15* and *IFIT-1* using SYBR premix ExTaq (Takara, Japan) according to the manufacturer's instruction. Each sample was assayed in triplicate with the 7500 Real-Time PCR system (Applied Biosystem, USA) for 40 cycles of 5 s at 95°C followed by 34 s at 60°C. The threshold cycle (Ct) is defined as the fractional cycle number at which the fluorescence passes the fixed threshold.

Pristane priming and AIFNα1bIgG01 treatment in mouse model

Balb/c mice around 6–8 weeks old were purchased from Shanghai SLAC Laboratory Animal comapany (Shanghai, China) and injected intraperitoneally (i.p.) with a single dose of 500 μl of pristane (2,6,10,14-tetramethylpentadecane, Sigma, USA) to establish a lupus-like mice model. Control mice were injected i.p. with 0.5 ml PBS. Sera were collected once every week to monitor the antibody production until 24 weeks. For antibody treatment, 200 μg AIFNα1bIgG01

antibodies were injected i.p. per mouse from 16th week after pristane treatment and continued for 4 weeks. Mice were killed at the 24th week. The total IgG and IgM antibodies in above mice sera were detected by ELISA. All the manipulation was performed in accordance with the experimental animal practice of Shanghai Jiaotong University School of Medicine.

Protein preparation

Gene fragment of human IFNα1b (amino acids 24–189) with N-terminal 6His-tag was amplified from human peripheral blood lymphocytes cDNA and cloned into pMCSG7 vector. The IFNα1b was produced in *Escherichia coli* BL21 (DE3). Cells were harvested and lysed by sonication in PBS (137 mM NaCl, 2.7 mM KCl, 50 mM Na_2HPO_4, 10 mM KH_2PO_4, pH 7.4). Soluble IFNα1b was purified by Ni affinity chromatography. After removal of imidazole, His-tag was removed by treating the protein with TEV protease. The tag-less protein was exchanged into a 20 mM Tris–HCl buffer, pH 7.5, using Superdex G75 (GE healthcare, USA) column. ScFv antibody AIFNα1bScFv01 expression and purification was done as described by Gong et al. [18]. The complex was formed by mixing equal molar amounts of AIFNα1bScFv01 with IFNα1b. The purity of the proteins was monitored by SDS-PAGE. The complex protein (15–20 mg/ml determined by NANODROP 2000 (Thermo scientific, USA)) was immediately screened for crystallization.

Crystallization and data collection

Crystallization screening was carried out using commercially available sparse matrix screens. 2 μl hanging drops containing 1 μl protein mixed with 1 μl mother liquor were equilibrated over 300 μl reservoir solution and incubated at 16°C. Crystals grew in magnesium acetate, 0.1 M Tris (pH 8.5), 12% PEG 8000 were flash frozen directly in liquid nitrogen without any cryo-protectant treatment prior to mounting and data collection at cryogenic temperature (100 K). The crystal diffracted X-rays to 2.8 Å at beamline 19-ID of APS, Argonne National Lab, US. The crystals belonged to space group C2 with unit cell dimensions: a=236.23 Å, b=91.95 Å, c=43.63 Å; α=90.00, β=99.75, γ=90.00.

Structure determination and refinement

Crystals were frozen in liquid nitrogen prior to diffraction testing and data collection. Native diffraction data were collected at a wavelength of 0.9794 Å. Data were indexed and scaled to 2.8 Å resolution using HKL2000 [19]. The structure was solved by the molecular replacement method using Balbes [17] automatically using 2JB5 [20] for light chain, 3KDM [21] for heavy chain, 1B5L [22] for IFNα1b as search models. The initial phases were improved with OASIS [23]. The model was manually improved in Coot [24]. Refinement was carried out using REFMAC [25] and PHENIX [26] alternately. TLS method embedded PHENIX was used in the final stage of the refinement [26]. Details of data collection and refinement statistics are listed in Table 1. The quality of the final model was validated with MolProbity [27].

Mutagenesis

Mutagenesis was designed to validate the epitopes of AIFNα1bIgG01 on IFNα1b unveiled by the crystal structure. Mutagenesis was carried out using QuikChange site-directed mutagenesis kit (Stratagene, USA) following the manufacturer's instructions. Mutants were expressed, purified, and assayed under identical conditions as the wild-type IFNα1b. The interaction between mutants of IFNα1b and

Table 1 Data collection and refinement statistics

Statistic	Antigen–antibody complex
Data collection	19-ID, APS
Wavelength(Å)	0.9794
Space group	C2
Cell dimensions	
a, *b*, *c* (Å)	236.23, 91.95, 43.63
α, β, γ (°)	90.00, 99.75, 90.00
Resolution (Å)	50.00–2.75 (2.82–2.75)
R_{sym} (%)	8.7 (40.2)
Mean I/σI (I)	12.00 (2.95)
Completeness (%)	99.9 (99.6)
Redundancy	3.7 (3.5)
Refinement	
Resolution (Å)	42–2.80
Reflections	21,633 (2,337)
R_{work}/R_{free} (%)	18.02/23.19 (23.89/30.96)
Atoms	
Protein	5,579
Water	87
Mean B value (Å^2)	26.57
R.m.s deviations	
Bonds (Å)	0.004
Angles (°)	0.60
Ramachandran analysis	
Favored region (%)	665 (95.00)
Allowed region (%)	31 (4.43)
Outliers (%)	4 (0.57)

Numbers in parentheses describing resolutions are statistics for the highest resolution shell

antibody were determined by Western blotting and ELISA as mentioned above.

Ethical Considerations

All studies involved in human samples has been approved by the ethics committee and the institutional review board of Shanghai Ruijin Hospital with written consents. The protocols for animal tests have been approved by animal care committee of Shanghai Jiaotong University

Accession code

The atomic coordinates and structure factors file of the human IFNα1b and AIFNα1bScFv01 complex have been deposited in the Protein Data Bank under the accession code 3UX9.

Results

Generation and functional characterization of a fully human antibody to IFNα1b

A single-chain antibody AIFNα1bScFv01 was first obtained by panning and screening a fully synthetic human antibody phage display library [18, 28], and converted to whole IgG antibody AIFNa1bIgG01. The human antibody specifically recognized IFNα1b but not recombinant IFNα2b or IFNγ as determined by Western blotting (Fig. 1a). The affinity (K_D) and kinetic rate constants for the binding of AIFNα1bIgG01 to immobilized IFNα1b were determined as 0.747 nM through SPR analysis (Fig. 1b), which was significantly higher than that reported for IFNα with its receptor IFNAR2 (100 nM) [29].

To determine whether AIFNα1bIgG01 could functionally block the bioactivity of IFNα, we tested the expression levels of type I ISGs, *ISG15* and *IFIT-1* in PBMCs from both SLE patients and healthy donors. We found that the expression of *ISG15* and *IFIT-1* in SLE patients was dramatically elevated when compared with healthy donors ($p<0.001$ for both genes; Fig. 2a). We further carried out ex vivo stimulation of PBMCs from 10 healthy donors by recombinant IFNα1b with or without AIFNα1bIgG01. The up-regulated expression level of *ISG15* and *IFIT-1* in PBMCs induced by IFNα1b were inhibited in a dose-dependent manner after adding series dilutions of the human antibody (Fig. 2b). We next wanted to figure out whether AIFNα1bIgG01 could neutralize the bioactivity of the IFNα existing in SLE patients' sera. High level of IFNα in 38 SLE patients' sera was detected in comparison with the sera from 23 healthy donors ($p<0.01$; Fig. 2c). The expression of *ISG15* in normal PBMCs was up-regulated by incubation with both recombinant IFNα1b

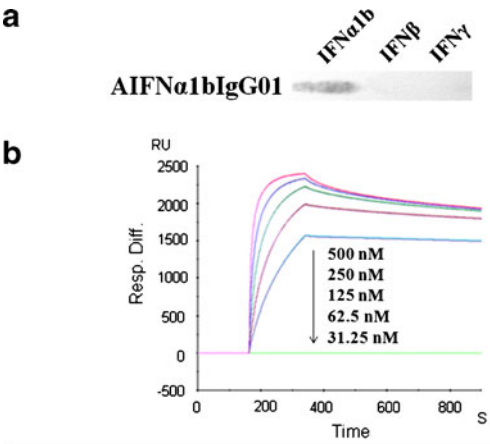

antibody	K_a ($\times 10^4$)$M^{-1}S^{-1}$	K_d ($\times 10^{-4}$)S^{-1}	K_D (K_d/K_a) nM
AIFNα1bIgG01	24.7	1.79	0.747

K_a: Association rate constant; K_d: Dissociation rate constant; K_D: Equilibrium dissociation constant

Fig. 1 AIFNα1bIgG01 recognizes human IFNα1b specifically. **a** Purified human IFNα1b, IFNα2b and IFNγ were probed with AIFNα1bIgG01. **b** Affinities for a range of concentrations of AIFNα1bIgG01 were measured on BIAcore 3000 using sensor chip CM5 immobilized with human IFNα1b. Each measurement represents an average of three independent assays that vary by 20%

(+IFNα) and SLE patients' sera (+PS1 and +PS2) but not the healthy donors' sera (+NS1 and +NS2; $p<0.001$). While adding the antibody AIFNα1bIgG01 during incubation, the expression level of *ISG15* was back to a base line compared with normal sera or media control groups (Fig. 2d).

To further evaluate the function of the antibody AIFNα1bIgG01 in vivo, we treated pristane-induced Balb/c mice with AIFNα1bIgG01 four times with 1 week interval. As showed in Fig. 2e, for the pristane-primed mice group without antibody treatment, the levels of total IgG and IgM antibodies in the sera started to elevated from the second month and remained at a high level until the mice were killed. However, with the treatment of AIFNα1bIgG01 started from the fourth month, both total IgG and IgM antibody levels in mice sera decreased at 1 month after treatment and kept at a relatively lower level when compared to PBS-treated pristane-primed mice. The results demonstrated that the intervention with AIFNα1bIgG1 antibody resulted in the partial remission of lupus-like pathogenesis in pristane-primed mice.

Determination of the crystal structure of the antibody and antigen binary complex

To delineate the structural basis for the inhibition of IFNα mediated signaling response by AIFNα1bIgG01, we determined the crystal structure of the binary complex of single-chain antibody of AIFNα1bIgG01 (termed as AIFNα1bScFv01) with the recombinant IFNα1b. The final

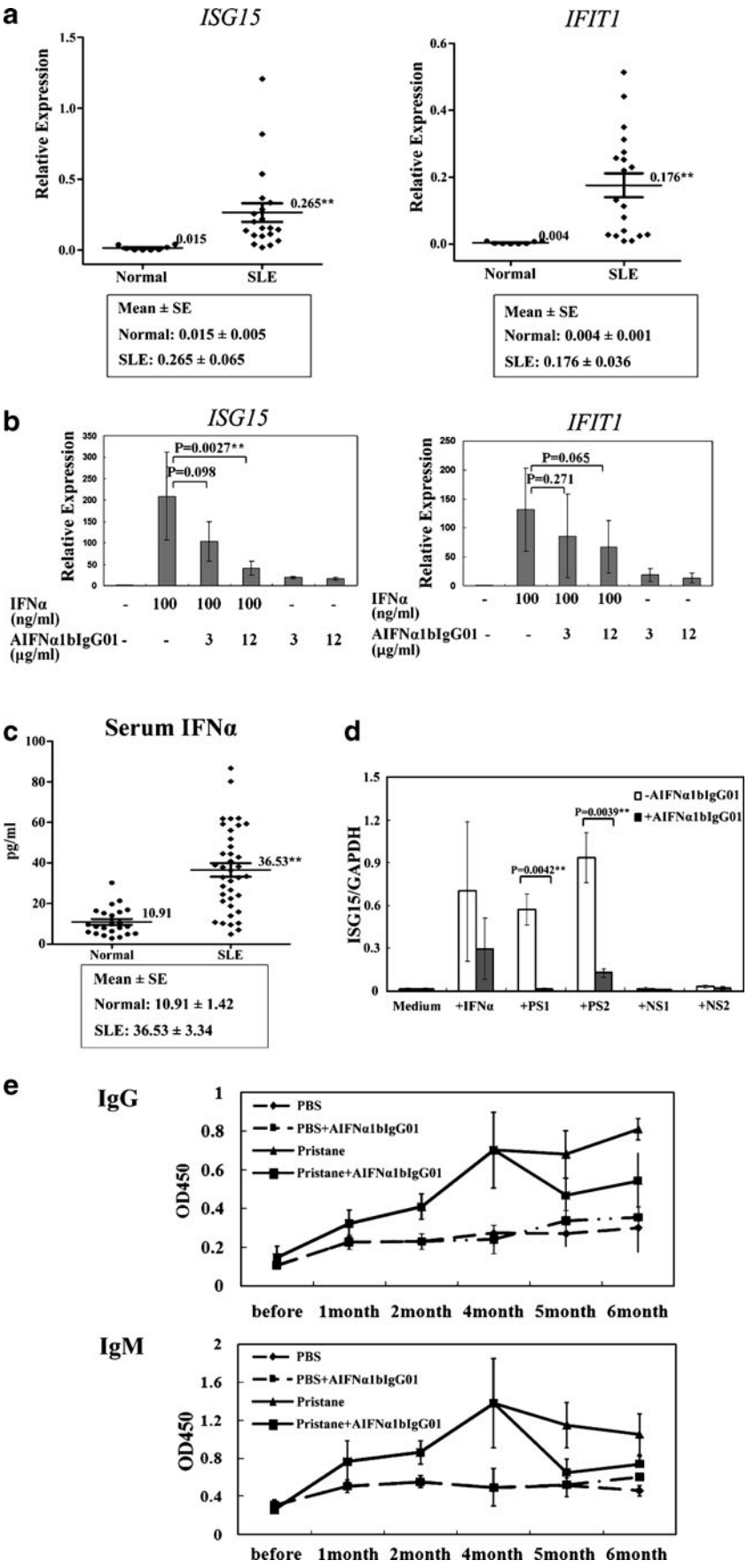

Fig. 2 Human antibody AIFNα1bIgG01 neutralized the bioactivity of IFNα1b. **a** The expression of *ISG15* and *IFIT-1* in PBMCs from SLE patients (n=20) and health donors (n=8) at $^{**}P<0.01$. Relative expression=$2\Delta Ct^{(ISG15/IFIT\text{-}1)\text{-}\Delta Ct(GAPDH)}$. **b** Overexpression of *ISG15* and *IFIT-1* in normal PBMCs (n=10) induced by human IFNα1b (100 ng/ml; *Line 1 from left*) and a dose-dependent neutralization by adding 3 ng/ml and 12 ng/ml of AIFNα1bIgG01(*Line 2–3 from left*) at $^{**}p<0.01$. AIFNα1bIgG01 only (*lines 4–5*) without IFNα1b. **c** Detection of the IFNα level in serum samples from SLE patients (N=38) and normal healthy donors (N=23; $^{**}p<0.01$). **d** Neutralization of activity of IFNα from SLE patients' sera with AIFNα1bIgG01. The expression of *ISG15* in normal PBMCs was up-regulated by IFNα (as positive control) and sera from SLE patients (+PS1 and +PS2), but not normal human sera (+NS1 and +NS2), while adding AIFNα1bIgG01 significantly down-regulated *ISG15 expression in* SLE patients ($^{**}p<0.01$). **e** AIFNα1bIgG01 decreased production of total IgG and IgM antibodies in the sera of pristane-primed lupus-like mouse model. The pristane-induced Balb/c mice were treated with AIFNα1bIgG01 (200 μg) started on the fourth month, four times with 1 week interval

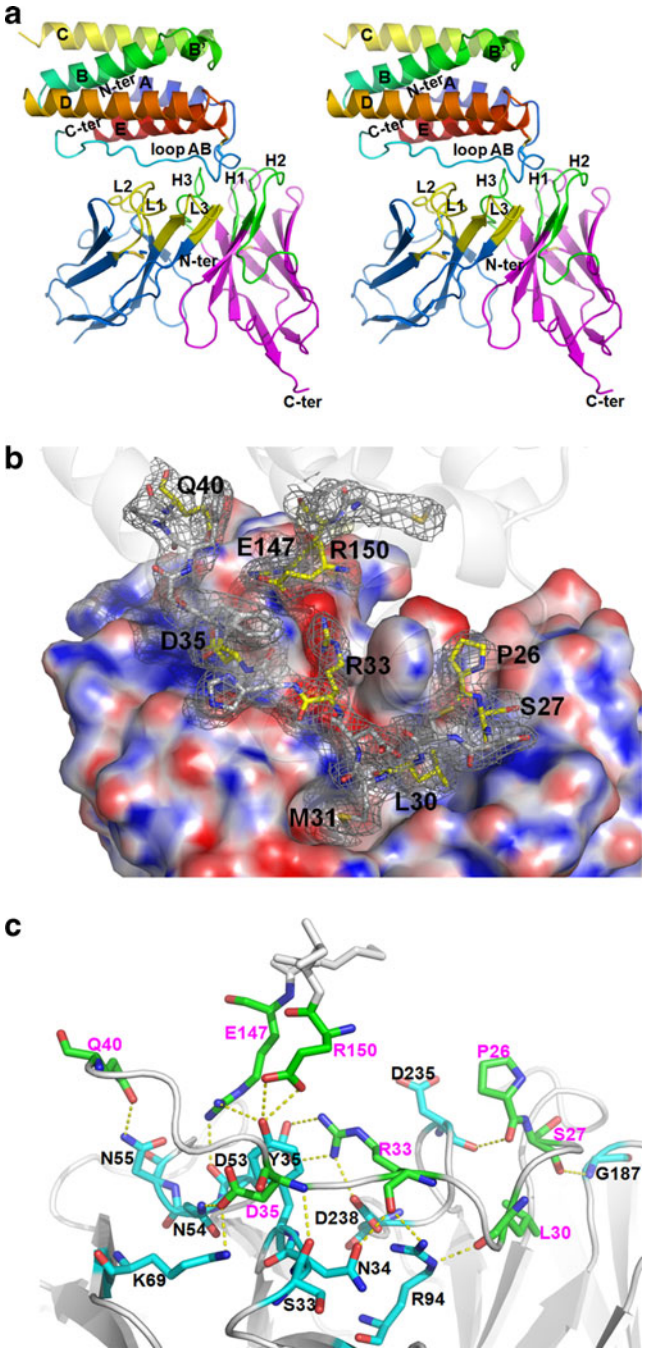

Fig. 3 Structure of the AIFNα1bScFv01-IFNα1b complex. **a** Stereo view of cartoon representation of human IFNα1b (*rainbow*) bound to AIFNα1bScFv01 (*light chain colored marine-blue*, heavy chain colored magenta). The CDRs were labeled and colored *yellow* in VL-CDR and *green* in VH-CDR. The N- and C- terminals were labeled N-ter and C-ter respectively. **b** Close up view of the interface between IFNα1b and AIFNα1bScFv01. Residues from IFNα1b loop AB region (P26-Q40) and helix E region (E147-R150) were shown as sticks representation. Interacting residues from IFNα1b were shown in *yellow*. Electron density of a 2Fo-Fc omit map for these residues at the interface of the IFNα1b-AIFNα1bScFv01 complex contoured at 1.0 σ. Met31 and Arg33 depict examples of shape and charge complementarity, respectively. AIFNα1bScFv01 was shown as electrostatic potential surface. *Blue* represents positive potential, *red* negative potential. Selected key residues were labeled. **c** Details of the AIFNα1bScFv01-IFNα1b complex interactions. Hydrogen bonds are shown as *yellow dashed lines*. Interacting residues from IFNα1b were shown in *green* and were labeled (*magenta*). Interacting residues from AIFNα1bScFv01 were shown in *cyan* and were labeled (*black*)

model has been refined to 2.8 Å resolution with a R_{cryst} and R_{free} factor values of 18.02% and 23.19%, respectively. Final refinement statistics are summarized in Table 1. The model contains residues 9–156 of the mature IFNα1b and residues 4–253 of AIFNα1bScFv01 (Fig. 3a). The final 2Fo-2Fc electron density map (Fig. 3b) is of good quality for most of the complex with the exception of two stretches of IFNα1b corresponding to residues 44–51 and 102–112 with weak electron density. Neither are the residues 113–135 of AIFNα1bScFv01 that comprise the linker region of heavy and light chain well defined in the electron density indicating disorder in this region.

Structural overview of AIFNα1bScFv01-IFNα1b complexes

The structure of IFNα1b (Fig. 3a) consists of five α helices (A–E) and a long loop connecting helix A with B (loop AB) in a tight bundle by predominantly hydrophobic interactions. Helices B, C and D are stacked up against helices A, E, and loop AB, respectively. The core at one (lower) end of the bundle is populated by aromatic amino acid residues such as Phe68, Trp77, Phe85, Phe124, Tyr130, and Trp141, which are involved in hydrophobic interactions. The side chain of Met21 from helix A is engaged in aryl-sulfur interactions with the π-electron cloud of the aromatic rings of Phe68, Phe85, and Trp77, which contributes to the stabilization of the core structure. As observed in other types of interferon, Cys29 from loop AB forms a disulfide bond with Cys139 from helix E.

AIFNα1bScFv01 folds into a typical β-sandwich immunoglobulin fold. The structure is bi-modular with the residues Ile4-Leu112 forming the light chain and Val136-Glu253 for the heavy chain (Fig. 3a). The binding site of AIFNα1bScFv01 is formed by the six complementarity determining regions (CDRs) and all the CDR regions project from the β-strands of VH and VL domains and display the canonical conformation, making it more feasible to provide steric or chemical complementarity with the antigen (Fig. 3a). More importantly, residues from CDRL3, H1, H2, and H3 form a concave cavity while the residues from CDRL1 and CDRL2 form a spherical pocket. These pockets and cavities probably offer binding sites for the epitopes of IFNα1b in the complex.

Shape complementarity and intermolecular ionic interactions underlies the high affinity of AIFNα1bScFv01 to human IFNα1b

The neutralization capacity of AIFNα1bScFv01 against human IFNα1b relies on its high binding affinity. The structure of the AIFNα1bScFv01-IFNα1b binary complex displayed three distinct regions at the interface that contribute to the binding of IFNα1b with AIFNα1bScFv01 via shape complementarity (Sc value, 0.788 calculated by sc 2.0 [30] in CCP4). In each instance, a side chain protrudes out into a cavity formed by its binding partner. IFNα1b contributes two such cavities that are separated by a third cavity formed by AIFNα1bScFv01. The two proteins are firmly zipped together with the side chains localized in these cavities. For instance, Tyr35 from AIFNα1bScFv01 protrudes inside a cavity formed by Arg33, His34, Asp35, Phe36, Gln40, Glu147, and Arg150 of IFNα1b. The IFNα1b Arg33 is engaged in the formation of a salt bridge with Asp53 of AIFNα1bScFv01 such that the aromatic ring of Tyr35 is positioned above the salt bridge. The second cavity is formed by residues Arg94, Asn96, Asn99 and Trp101 of AIFNα1bScFv01 with the side chain of Met31 from IFNα1b localized in the center of the cavity (Fig. 3b). The side chain of Met31 is involved in aryl-π interactions with Trp101 of AIFNα1bScFv01 and numerous van der Waal's interactions with the amino acid residues forming the cavity. Finally, the side chain of Phe236 is trapped inside a cavity formed by Pro26, Cys29, Asp32, Arg33, Glu142, Val143, and Ala146 of IFNα1b.

In addition to shape complementarity, intermolecular ionic interactions between AIFNα1bScFv01 and IFNα1b stabilize the interface. Totally 11 amino acid residues from the AIFNα1bScFv01 and 8 amino acid residues from IFNα1b form 16 pairs of hydrogen bonds as summarized in Table 2 and Fig. 3c. Most of the residues engaged are localized in the CDR regions of AIFNα1bScFv01 and loop AB/helix E domain of IFNα1b, respectively.

Table 2 Summary of the interface residues and hydrogen bond interactions no more than 3.3 Å in the ScFv-IFNα1b complex

Chain	ScFv contact atom	IFNα1b contact atom	Length (Å)
VL			
CDRL1	Ser33 O	Asp 35 (loop AB) N	3.1
	Asn34 O	Arg 33 (loop AB) O	2.9
	Tyr35 O	Glu147 (helix E) O	3.1
	Tyr35 O	Glu147 (helix E) O	3.0
	Tyr35 O	Arg150 (helix E) N	3.3
CDRL2	Asp53 O	Arg33 (loop AB) N	3.2
	Asp53 O	Arg33 (loop AB) N	2.9
	Asp53 O	Arg150 (helix E) N	3.3
	Asn54 N	Asp35 (loop AB) O	2.7
	Asn55 N	Gln40 (loop AB) O	3.0
CDR L3	Arg94 N	Leu30 (loop AB) O	2.8
	Arg94 N	Arg33 (loop AB) O	3.0
VH			
CDRH2	Gly187 N	Ser27 (loop AB) O	3.2
CDRH3	Asp235 O	Pro26 (loop AB) O	3.3
CDRH3	Asp238 O	Arg33 (loop AB) N	3.0
Non-CDR[a]	Lys69 N	Asp35 (loop AB) O	2.8

[a] In addition to the expected contacts from CDR loops in the ScFv, an additional residue from a non-CDR also interacts with IFNα1b

AIFNα1bScFv01 interacts with two hotspot regions anchoring on IFNα1b that mediates the initiation of IFNα signaling

IFNα1b-AIFNα1bScFv01 complex structure superimposed over IFNα2b-IFNAR2-EC structure indicated that these epitopes were partially overlapped with the binding sites of IFNα2 with IFNAR2 (Fig. 4a), which was necessary for the initiation of IFN signaling [29, 31–33]. We further mutated each amino acid of Pro26-Asp35 of IFNα1b to test the interaction with antibody AIFNα1bIgG01. The results showed that P26G, S27G, S28G, M31G, R33G and H34G mutations slightly reduced the binding efficiency, while D32G mutation greatly diminished the binding activity; L30G or D35G mutations completely abolished the binding of IFNα1b to AIFNα1bIgG01 (Fig. 4b). Q40A mutation in loop AB as well as E147D and R150A in helix E had no changes in Western blot assay (Fig. 4b bottom panel), but the binding property dramatically decreased for mutant R150A in ELISA assay, whereas mutant E147D showed no change in comparison with wild-type IFNα1b (Fig. 4c). The results indicated that the loop AB was necessary for the interaction of IFNα1b with AIFNα1bIgG01, in which Leu30, Asp32, Asp35, and R150 residues were particularly critical.

AIFNα1bScFv01 could recognize IFNα1b but not IFNα2b. We analyzed the interface of the AIFNα1bScFv01-IFNα1b binary complex alone and the structure superimposing IFNα2b over IFNα1b (Fig. 4a and d). We found that the binding of AIFNα1bScFv01 to human IFNα2b at AB loop was hindered due to steric clashes and chemical incompatibility; IFNα1b has a Ser27 and Met 31 at loop AB, while IFNα2b owns Phe 27 and Lys 31. Replacement of Ser27 with a phenylalanine would result in steric clashes and disrupt its interaction with Gly187 (Fig. 4d left panel). The side chain of Met31 is protruding inside a spherical cavity formed by Arg94, Asn96, Asn99 and Trp101 of AIFNα1bScFv01. Substitution of Met 31 with lysine residue could result in a repulsion of the side chain by the

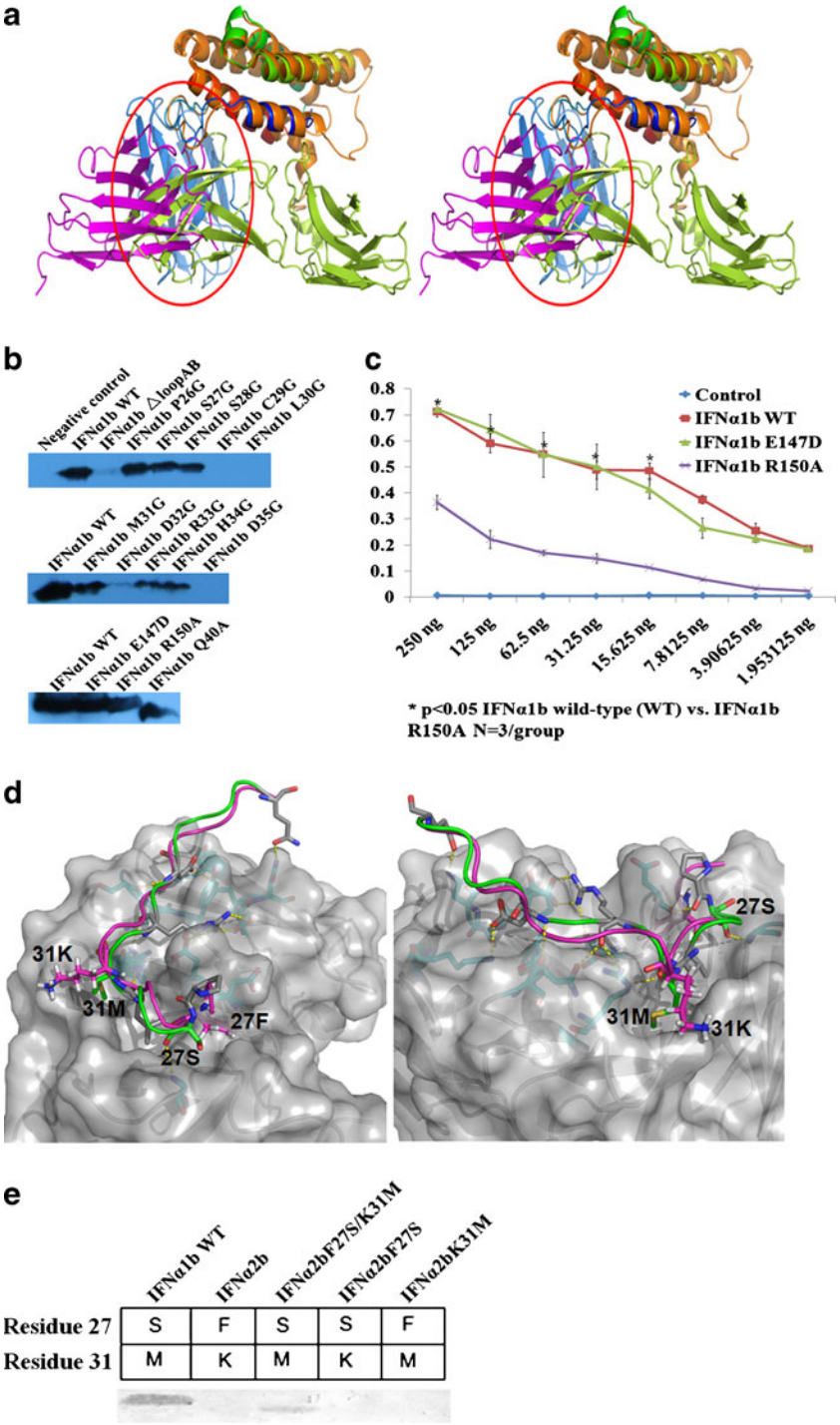

guanidium nitrogens of Arg94 and δ2 N atom of Asn99, preventing the association of AIFNα1bScFv01 with IFNα (Fig. 4d right panel). Mutagenesis studies further confirmed the importance of Ser27 and Met31 in conferring antigenic specificity. A double mutation (F27S and K31M) of IFNα2b resulted in binding of IFNα2b to AIFNα1bScFv01 (Fig. 4e).

Discussion

In this report, for the first time, we described a high affinity neutralizing human antibody AIFNα1bIgG01 and revealed the molecular basis for its interaction with human IFNα2b through a antigen–antibody crystal structure in complex. The antibody, through competition with IFNAR2 to bind

◀ **Fig. 4** Comfirmation of the antibody binding epitopes. **a** Stereo view of IFNα1b-AIFNα1bScFv01 complex (the same color schema as shown in Fig. 3a) superimposed over IFNα2b-IFNAR2-EC (orange for IFNα2b and limon for IFNAR2-EC, PDB code 2KZ1). Typical steric hindrance regions were highlighted in *red circles*. **b** The binding of AIFNα1bIgG01 with wild-type IFNα1b and its mutants. Mutants from loop AB including 26-PSSCLMDRHD-35 as well as Q40A, E147D and R150A, were tested for its ability to interact with AIFNα1-bIgG01 in a Western blotting assay. **c** Comparison of AIFNα1bIgG01 antibody binding avidity to wide type (IFNα1bWT) and mutated IFNα1b (IFN1bE147D, R150A) by ELISA as described in the "Methods" section. **d** Phe27 clashed sterically (*left panel*), while Lys31 was chemically incompatible (*right panel*) when amino acids spanning Leu26-Gln40 of the loop AB region of IFNα2b (*magenta*) were superimposed over the AIFNα1bScFv01-IFNα1b complex. Equivalent residues of IFNα1b (*green*) have been shown for comparison. AIFNα1bScFv01 was depicted in *gray* surface with 40% transparency. Eleven interacting residues were shown as sticks in cyan carbons. Hydrogen bonds between AIF-Nα1bScFv01 and IFNα1b were shown as *yellow dashed line*. **e** The effect of mutating residues 27 and 31 of IFNα1b and IFNα2b on the binding of antibody AIFNα1bIgG01 was tested by Western blotting assay. Wild-type IFNα1b binds AIFNα1bIgG01 strongly. Wild-type IFNα2b, has a phenylalanine and a lysine at positions 27 and 31, respectively, and could not bind AIFNα1bIgG01. Double mutant IFNα2b F27S/K31M could bind AIFNα1bIgG01 weakly when compared to the wild-type IFNα1b. Single-point mutant IFNα2b F27S could not bind AIFNα1bIgG01. Similarly, single-point mutant IFNα2b K31M could not bind AIFNα1bIgG01

with IFNα, could down-regulate the expression of signaling molecules *ISG15* and *IFIT-1*in interferon pathway, and block the bioactivity of IFNα in vitro and in vivo.

Recent reports strongly suggest that type I IFNs are involved in the pathogenesis of SLE and other autoimmune syndromes [7], however, little is known about the epitope of IFN that participates in the pathogenesis of SLE. The high-resolution structure models we described in this report clearly showed the molecular details of the interaction between the antibody and antigen, and giving clear picture of antibody binding epitope, both Pro26-Gln40 region in loop AB and Glu147-Arg150 region in helix E of IFNα1b contribute to the antibody binding, and four residues of above two regions (Leu30, Asp32, Asp35, and Arg150) are critical for the formation of antigen-antibody complexes. The results is also consistent with a previous reported epitope residues 22–31 recognized by another IFNα targeted human neutralizing antibody [34].

In order to gain insights into the nature of the IFNα1b epitope, we looked at the structure of IFNα2b bound to the IFNAR2 receptor. Previously, IFNα2b was shown to bind its receptor IFNAR2 primarily via the loop AB region and helices A and E. Although, IFNα2b shares 83% sequence identity with IFNα1b, AIFNα1bIgG01 specifically binds IFNα1b but not IFNα2b. We compared the epitope sequences in loop AB and helix E between IFNα1b and IFNα2b, only residues Ser 27 and Met 31 were different, and these two amino acids contributed to the specificity of the antibody (Fig. 4). In fact, the interaction of IFNα with its receptors IFNAR1/IFNAR2 presented as a heterotrimeric architecture, the subtypes of IFNα interact with receptors in a very conserved way. Leu30 and Asp32 residues are conserved in all the subtypes of type I interferons and are critical in the interaction between IFN and IFNAR2 [32]. These two anchor points are also engaged in the interaction in the binary complex of AIFNα1bScFvG01-IFNα1b, which provides sufficient evidence that AIFNα1bIgG01 targets a conserved epitope of type I interferon engaged in the initiation of IFN signaling. This may also help to interpret the observation that AIFNα1bIgG01 efficiently neutralizes the bioactivity of interferon derived from the patients' sera which contain different subtypes of type I interferons.

In conclusion, through determining the crystal structure of AIFNα1bScFv01 in complex with recombinant IFNα1b, we have dissected the structural basis of the inhibitory function of the human antibody against IFNα1b as well as characterized the epitopes of the antibody harboring on IFNα for the first time. AIFNα1bIgG01 sequesters the IFNα1b epitope with high affinity to block the interaction of IFNα with its receptor IFNAR2, which results in the impairment of up-regulation of ISGs in the IFNα signaling pathway. These results highlight the tremendous potential of recombinant human antibody treatment strategy for human SLE. In addition, the definition of the critical epitope provides new insights for the development of effective targeted drug to prevent the over immune regulation induced by the increase of IFNα in various autoimmune disease.

Acknowledgements This work was funded by the Ministry of Science and Technology of China (grants 2009AA02Z109, 2009DFB30310 and 2009CB918803) and National Nature Science Foundation of China (grants 31070660, 31021062 and 81072449); Crystallographic data were collected at beamline 19-ID of APS (Argonne National Laboratory)

Disclosure statement The authors declare no conflict of interest in connection with the submitted material.

References

1. Giffords ED (2003) Understanding and managing systemic lupus erythematosus (SLE). Soc Work Health Care 37:57–72
2. Lahita R (1999) The clinical presentation of systemic lupus erythematosus. Academic, San Diego
3. Flesher DL, Sun X, Behrens TW, Graham RR, Criswell LA (2010) Recent advances in the genetics of systemic lupus erythematosus. Expert Rev Clin Immunol 6:461–479
4. Obermoser G, Pascual V (2010) The interferon-alpha signature of systemic lupus erythematosus. Lupus 19:1012–1019
5. Rahman A, Isenberg DA (2008) Systemic lupus erythematosus. N Engl J Med 358:929–939
6. Ronnblom L, Elkon KB (2010) Cytokines as therapeutic targets in SLE. Nat Rev Rheumatol 6:339–347
7. Banchereau J, Pascual V (2006) Type I interferon in systemic lupus erythematosus and other autoimmune diseases. Immunity 25:383–392

8. Pascual V, Farkas L, Banchereau J (2006) Systemic lupus erythematosus: all roads lead to type I interferons. Curr Opin Immunol 18:676–682
9. Ronnblom L, Alm GV, Eloranta ML (2009) Type I interferon and lupus. Curr Opin Rheumatol 21:471–477
10. Bennett L, Palucka AK, Arce E, Cantrell V, Borvak J, Banchereau J, Pascual V (2003) Interferon and granulopoiesis signatures in systemic lupus erythematosus blood. J Exp Med 197:711–723
11. Reddy MV, Velazquez-Cruz R, Baca V, Lima G, Granados J, Orozco L, Alarcon-Riquelme ME (2007) Genetic association of IRF5 with SLE in Mexicans: higher frequency of the risk haplotype and its homozygozity than Europeans. Hum Genet 121:721–727
12. Kim T, Kanayama Y, Negoro N, Okamura M, Takeda T, Inoue T (1987) Serum levels of interferons in patients with systemic lupus erythematosus. Clin Exp Immunol 70:562–569
13. Pascual V, Allantaz F, Patel P, Palucka AK, Chaussabel D, Banchereau J (2008) How the study of children with rheumatic diseases identified interferon-alpha and interleukin-1 as novel therapeutic targets. Immunol Rev 223:39–59
14. Chuntharapai A, Lai J, Huang X, Gibbs V, Kim KJ, Presta LG, Stewart TA (2001) Characterization and humanization of a monoclonal antibody that neutralizes human leukocyte interferon: a candidate therapeutic for IDDM and SLE. Cytokine 15:250–260
15. Sheets MD, Amersdorfer P, Finnern R, Sargent P, Lindquist E, Schier R, Hemingsen G, Wong C, Gerhart JC, Marks JD (1998) Efficient construction of a large nonimmune phage antibody library: the production of high-affinity human single-chain antibodies to protein antigens. Proc Natl Acad Sci U S A 95:6157–6162
16. Liang M, Dübel S, Li D, Queitsch I, Li W, Bautz EK (2001) Baculovirus expression cassette vectors for rapid production of complete human IgG from phage display selected antibody fragments. J Immunol Methods 247:119–130
17. Long F, Vagin AA, Young P, Murshudov GN (2008) BALBES: a molecular-replacement pipeline. Acta Crystallogr D: Biol Crystallogr 64:125–132
18. Gong B, Wang S, Li C, Wang Y, Zhang Q, Chen Z, Sun L, Liang M, Sun Z, Li D (2009) Antibody against human interferon alb from human synthetic recombinant antibody library. Chin Med Biotechnol 4:184–189 [in Chinese]
19. Otwinowski ZMW (1997) Processing of X-ray diffraction data collected in oscillation mode. Academic, New York
20. Hillig RC, Urlinger S, Fanghanel J, Brocks B, Haenel C, Stark Y, Sulzle D, Svergun DI, Baesler S, Malawski G et al (2008) Fab MOR03268 triggers absorption shift of a diagnostic dye via packaging in a solvent-shielded Fab dimer interface. J Mol Biol 377:206–219
21. Niemi MH, Takkinen K, Amundsen L, Söderlund H, Rouvinen J, Höyhtyä M (2010) The testosterone binding mechanism of an antibody derived from a naïve human scFv library. J Mol Recog 24:209–219
22. Radhakrishnan R, Walter LJ, Subramaniam PS, Johnson HM, Walter MR (1999) Crystal structure of ovine interferon-tau at 2.1 Å resolution. J Mol Biol 286:151–162
23. He Y, Yao DQ, Gu YX, Lin ZJ, Zheng CD, Fan HF (2007) OASIS and molecular-replacement model completion. Acta Crystallogr D: Biol Crystallogr 63:793–799
24. Emsley P, Lohkamp B, Scott WG, Cowtan K (2010) Features and development of Coot. Acta Crystallogr D: Biol Crystallogr 66:486–501
25. Murshudov GN, Vagin AA, Dodson EJ (1997) Refinement of macromolecular structures by the maximum-likelihood method. Acta Crystallogr D: Biol Crystallogr 53:240–255
26. Terwilliger TC, Grosse-Kunstleve RW, Afonine PV, Moriarty NW, Zwart PH, Hung LW, Read RJ, Adams PD (2008) Iterative model building, structure refinement and density modification with the PHENIX AutoBuild wizard. Acta Crystallogr D: Biol Crystallogr 64:61–69
27. Chen VB, Arendall WB 3rd, Headd JJ, Keedy DA, Immormino RM, Kapral GJ, Murray LW, Richardson JS, Richardson DC (2010) MolProbity: all-atom structure validation for macromolecular crystallography. Acta Crystallogr D: Biol Crystallogr 66:12–21
28. Du W, Wang S, Sun Z, Yu W (2006) Construction of a fully synthetic human phage display antibody library. Bull Acad Mil Med Sci 30(319–322):328 [in Chinese]
29. Jaks E, Gavutis M, Uze G, Martal J, Piehler J (2007) Differential receptor subunit affinities of type I interferons govern differential signal activation. J Mol Biol 366:525–539
30. Lawrence MC, Colman PM (1993) Shape complementarity at protein/protein interfaces. J Mol Biol 234:946–950
31. Quadt-Akabayov SR, Chill JH, Levy R, Kessler N, Anglister J (2006) Determination of the human type I interferon receptor binding site on human interferon-alpha2 by cross saturation and an NMR-based model of the complex. Protein Sci 15:2656–2668
32. Thomas C, Moraga I, Levin D, Krutzik PO, Podoplelova Y, Trejo A, Lee C, Yarden G, Vleck SE, Glenn JS et al (2011) Structural linkage between ligand discrimination and receptor activation by type I interferons. Cell 146:621–632
33. Yao Y, Richman L, Higgs BW, Morehouse CA, de los Reyes M, Brohawn P, Zhang J, White B, Coyle AJ, Kiener PA et al (2009) Neutralization of interferon-alpha/beta-inducible genes and downstream effect in a phase I trial of an anti-interferon-alpha monoclonal antibody in systemic lupus erythematosus. Arthritis Rheum 60:1785–1796
34. Nolte KU, Gunther G, von Wussow P (1996) Epitopes recognized by neutralizing therapy-induced human anti-interferon-alpha antibodies are localized within the N-terminal functional domain of recombinant interferon-alpha 2. Eur J Immunol 26:2155–2159